Astrophys. Space Sci. Trans., 8, 45–49, 2012
www.astrophys-space-sci-trans.net/8/45/2012/
doi:10.5194/astra-8-45-2012

Astrophysics and Space Sciences Transactions

In-field calibration of the Navigation Dosimetry System (NAVIDOS) during solar minimum conditions

T. Möller[1,2], O. Burda[2], S. Burmeister[1], B. Heber[1], F. Langner[2], and F. Wissmann[2]

[1]Christian-Albrechts-University (CAU), Institute of Experimental and Applied Physics, Leibnizstr. 11–19, 24118 Kiel, Germany
[2]Physikalisch-Technische Bundesanstalt (PTB), Bundesallee 100, 38116 Braunschweig, Germany

Correspondence to: T. Möller (tmoeller@physik.uni-kiel.de)

Received: 3 December 2012 – Revised: 11 April 2013 – Accepted: 3 May 2013 – Published: 24 June 2013

Abstract. The NAVIgation DOsimetry System (NAVIDOS) comprises a complete readout system for a radiation detector, an air pressure sensor and a GPS receiver. The detector system DOSTEL uses silicon detectors which make NAVIDOS light weighted and compact in size. Therefore, NAVIDOS is well suited to be installed on board aircraft. The calibration of NAVIDOS in terms of ambient dose equivalent is done by an in-field comparison with the PTB reference instrument πDOS. We also show that the dependence of these results on the vertical cut-off rigidity can be explained by the low response of the silicon detectors for neutrons. Therefore, in-flight measurements have been performed together with the PTB reference instrument πDOS. The dose rates, calculated using the PTB code FDOScalc, were verified with these πDOS measurements. The calibration of NAVIDOS was done with FDOScalc and results in calibration factors between 3.4 in the polar and 2.4 in the equator region.

1 Introduction

At flight altitudes the radiation field of secondary cosmic radiation is complex in terms of particle composition and energies. The neutral component includes mainly neutrons and photons, and the charged component comprises mostly protons, muons, electrons and pions.

Because of this it is difficult to measure the ambient dose equivalent. However, it has been shown that a tissue-equivalent proportional counter (TEPC) can approximately measure the ambient dose equivalent at cruising altitudes (Schrewe, 2000; Lewis, 2002; Wissmann, 2006). To investigate this radiation field the PTB Dosimetry System πDOS (Wissmann, 2006, 2004) was developed. It consists of a 2 inch TEPC installed in a cabin baggage sized suit case including all necessary electronic equipment to run the dosemeter system in a stand alone mode for about 12 hours. From December 2003 to September 2004 it was permanently installed in an aircraft (Wissmann, 2006) and measured ambient dose equivalent rates at flight altitudes mainly on routes between Frankfurt and North America. Since πDOS was well characterized in photon reference fields (according to ISO 4037, Büermann, 1999) and neutron reference fields (according to ISO 8592, Nolte, 2004), the results are traceable to the primary standards maintained by PTB.

Using previous measurements performed by PTB in the years 1997 to 1999 and all data measured with πDOS between 2003 and 2006 a mathematical description of the ambient dose equivalent rates as a function of latitude, longitude, altitude and solar activity has been developed and was implemented in the software code FDOScalc (Wissmann, 2010a). Solar activity is expressed in the software code by the count rate of the neutron monitor in Oulu, Finland (Usoskin, 2011; Oulu, 2008). The calculations are restricted to the ranges where the PTB measurements were done, i.e. at typical altitudes between flight level FL250 and FL400, and neutron monitor count rates between 5700 counts min^{-1} and 6500 counts min^{-1}. Within these constraints FDOScalc allows to calculate the reference values for ambient dose equivalent rates at any location in the atmosphere and for any phase in the solar activity cycle.

Because πDOS is too bulky in size and mass (more than 20 kg) to be used routinely on board passenger aircraft, the **Nav**igation **Do**semeter **S**ystem (NAVIDOS) has been developed. NAVIDOS is small in size (17 cm $\times$ 17 cm $\times$

Published by Copernicus Publications on behalf of the Arbeitsgemeinschaft Extraterrestrische Forschung e.V.

12 cm) and mass (about 4 kg) and utilizes among other the DOSimetry TELescope (DOSTEL) (Beaujean, 1999a, 2005) as dosemeter. For a full discription of DOSTEL see (Beaujean, 1999b). DOSTEL is based on a silicon detector stack. Thus, the material is not tissue equivalent and, therefore, the response to neutrons is rather poor due to the high Z. Because neutrons are the main part of the ambient dose equivalent at aviation altitudes (Bartlett, 2004), a careful in-field calibration was performed which used the ambient dose equivalent rates measured by πDOS and the ones calculated with FDOScalc as reference values.

2 Measurement flights

Measurements were conducted during two flights with different destinations. The first one was a flight across the equator from Frankfurt to Cape Town and back in November 2007. The second one was from Dusseldorf to Bangkok and back to Munich in September 2008. The flight to Bangkok was selected due to the high vertical cut-off rigidity along the flight path. Figure 1 shows a world map with the calculated effective vertical cut-off rigidities for an altitude of 20 km together with the flight routes. The effective vertical cut-off rigidity was calculated using Planetocosmics (L. Desorgher, personal communication, 2003). For this simulation the Tsyganenko89 model and the International Geomagnetic Reference Field (IGRF) with the parameters from 2005 were used (K. Herbst, personal communication, 2008). The changes of the parameters from 2005 to 2008 have no significant effect on the analysis of the data. In addition, we used the results of the CARAMEL measurement campaign in order to cover cut-off rigidities below 4 GV. These measurements were performed on a specific location in the south of Norway and in the south of Germany. The CARAMEL measurement campaign details can be found in (Wissmann, 2010b).

3 Calibration

NAVIDOS records the accumulated absorbed dose (energy deposition per mass) and the environment parameters cabin pressure and GPS coordinates every minute. The results of the dose rate measurements are shown in Fig. 2.

To convert the measured dose rates in Silicon into ambient dose equivalent rates, the NAVIDOS results are compared with the reference values calculated with FDOScalc, as shown by the solid line in Fig. 2. From that figure it is evident that the πDOS measurements are consistent with the FDOScalc results. It has already been shown in Ref. (Schrewe, 2000), that the ambient dose equivalent rate depends on the altitude and the cut-off rigidity R_c. This is also visible in Fig. 2 (left plot): the dose rate in silicon and the ambient dose equivalent rate increase when the aircraft changes it's flight altitude from FL330 to FL370 at flight time 375 on its way from Frankfurt to Cape Town. The slowly varying

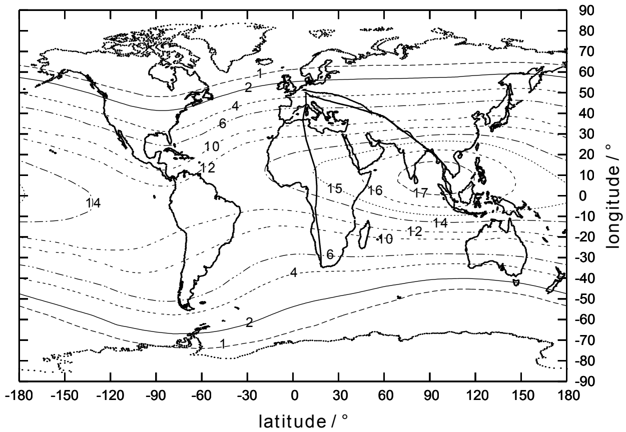

Fig. 1. Vertical cut-off rigidity contour plot for epoch 2005 at an altitude of 20 km together with the flight routes (thick solid lines) along which the measurements have been carried out.

dose rate is a consequence of the increasing and then decreasing cut-off rigidity.

The field calibration factor N_{field} is defined by the ratio of the FDOScalc calculated ambient dose equivalent rate $\dot{H}^*(10)_{\text{FD}}$, and the dose rate in Silicon $\dot{D}_{\text{Si}}$ measured by NAVIDOS:

$$N_{\text{field}}(R_c, h) = \frac{\dot{H}^*(10)_{\text{FD}}(R_c, h)}{\dot{D}_{\text{Si}}(R_c, h)} \quad (1)$$

Thus, in order to calculate the field calibration factor we use the measured altitude and calculate the vertical cut-off rigidity from the GPS information. Then the dose rate is averaged within a cut-off rigidity interval of 1 GV, assuming that the altitude dependence of the calibration factor is negligible. The result of the calibration for NAVIDOS is shown in Fig. 3. The calibration factors for $R_c < 4$ GV are taken from the CARAMEL campaign (Wissmann, 2010b).

The calibration factors show a strong dependence on the vertical cut-off rigidity R_c which can be approximated by

$$N_{\text{fit}}(R_c) = N_0 + \frac{N_1}{1 + e^{(R_c - R_1)/R_0}} \quad (2)$$

A fit of this function ($\chi^2 = 0.8$) to the calibration factors yields the following parameters:

$$\begin{aligned} N_0 &= 2.39 \pm 0.02 \qquad N_1 = 1.00 \pm 0.07 \\ R_1 &= 7.17 \pm 0.30\ \text{GV} \quad R_0 = 1.88 \pm 0.25\ \text{GV} \end{aligned} \quad (3)$$

where the given uncertainties are the 1σ standard uncertainty. Note that the extreme values vary between 2.4 at $R_c \gtrsim 14$ GV and 3.4 for $R_c \lesssim 2$ GV. The cut-off dependence of the calibration function can be explained by the low neutron detection efficiency of the silicon detector. As discussed in Sect. 4 the relative contributions of neutrons in the polar region is

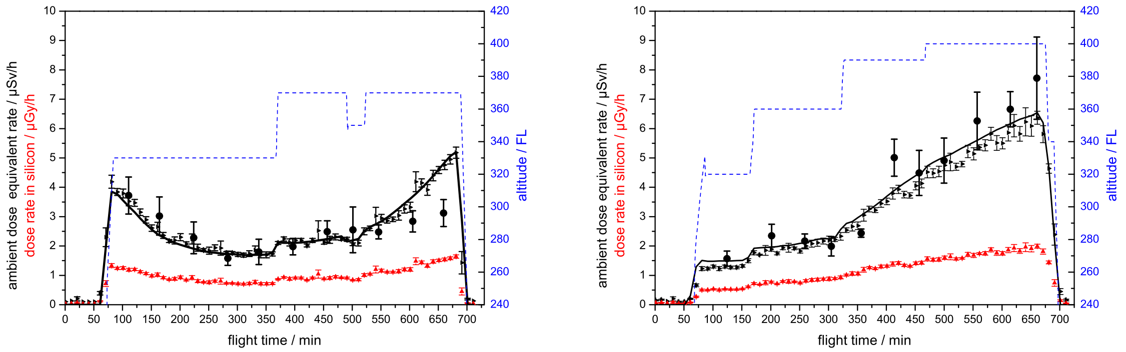

Fig. 2. Dose rate profiles for the flights from Frankfurt to Cape Town (left plot), and from Bangkok to Munich (right plot), taken from Möller (2008). Plotted are the dose rates in Silicon $\dot{D}_{\mathrm{Si}}$ (red ▲) measured by NAVIDOS and the calibrated values in terms of $\dot{H}^*(10)$ (▶). The πDOS results are given by the full circles (•) (Wissmann, 2010a) and the solid line is the calculation using FDOScalc. The dashed line displays the flown altitude in unit of flight level (right axis).

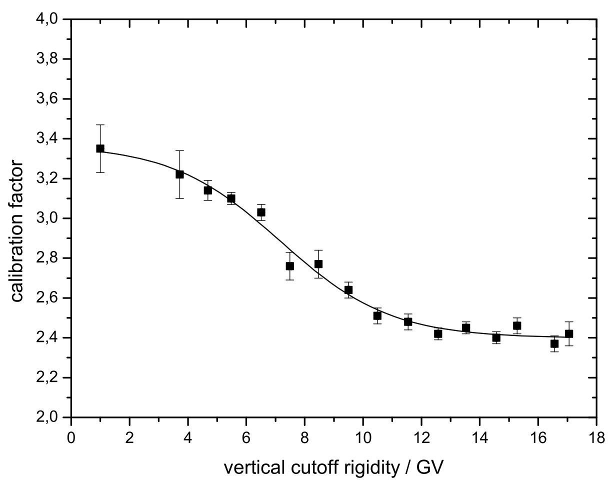

Fig. 3. Graphical display of the calibration function (Eq. 2) using the parameters as given in Eq. (3).

higher than in the equator region. Taking into account the response of silicon to different particle species (charged, neutrals) the calibration function corrects the measurements in order to obtain the dose rate. Thus, by this procedure the neutron component in the measured dose rate is corrected. Applying the calibration function to all measured dose rates yields the results as plotted in Fig. 2. The plot also shows that changes in flight altitudes which were neglected in the determination of N_{fit} are reproduced. The good agreement of the NAVIDOS data with the ones from πDOS confirms the validity of the calibration procedure.

4 Discussion

The calibration function in Eq. (2) is, of course, determined by FDOScalc. That in turn means, that the validity of FDOScalc is assumed. As mentioned above, FDOScalc represents a mathematical description of the TEPC measurements. Therefore, possible deviations of these measurements from the apriori unknown true values, although assumed to be small, can influence the calibration function. The calibration function $N_{\mathrm{fit}}(R_{\mathrm{c}})$ can be assumed to be factorized into two factors:

$$N_{\mathrm{fit}}(R_{\mathrm{c}}) = F_{\mathrm{Si-water}} \cdot C_{\mathrm{field}}(R_{\mathrm{c}}). \quad (4)$$

Beaujean (2005) and Roos (1997) showed that the dose rate in silicon can be converted into dose in water by using a conversion factor $F_{\mathrm{Si-water}} = 1.20$. This factor considers the different stopping power (deduced for electrons (ICRU, 1984)) of charged particles in water and silicon. Note, that Benton (2010) showed that $F_{\mathrm{Si-water}}$ depends on the LET of the particle. The factor $C_{\mathrm{field}}(R_{\mathrm{c}})$ in Eq. (4) is a function of the cut-off rigidity R_{c} and, therefore, is determined by the radiation field.

In order to investigate the calibration factor further we compare the contributions of charged and neutral particles to the ambient dose equivalent rate by utilizing the Excel-based Program for calculating the atmospheric cosmic-ray spectrum (EXPACS) based on the PARMA code (Sato, 2006, 2008).

Figure 4 shows the radiation field components which contribute to the ambient dose equivalent rate at FL350 near solar minimum conditions ($\Phi = 350$ MV), as calculated with EXPACS as function of R_{c}. The contribution of photons to the dose equivalent rate is below 5 % for all vertical cut-off rigidities (dashed line in Fig. 4 left). Neutrons contribute about 65 % for $R_{\mathrm{c}} < 3$ GV. From $R_{\mathrm{c}} = 3$ GV to $R_{\mathrm{c}} = 12$ GV a rather strong dependence on the vertical cut-off rigidity exists. The solid line in Fig. 4 shows the calculated percentage of the secondary charged particle component to the total dose at FL350 for R_{c} between 0 and 17 GV. This ratio increases from 34 % to 52 %.

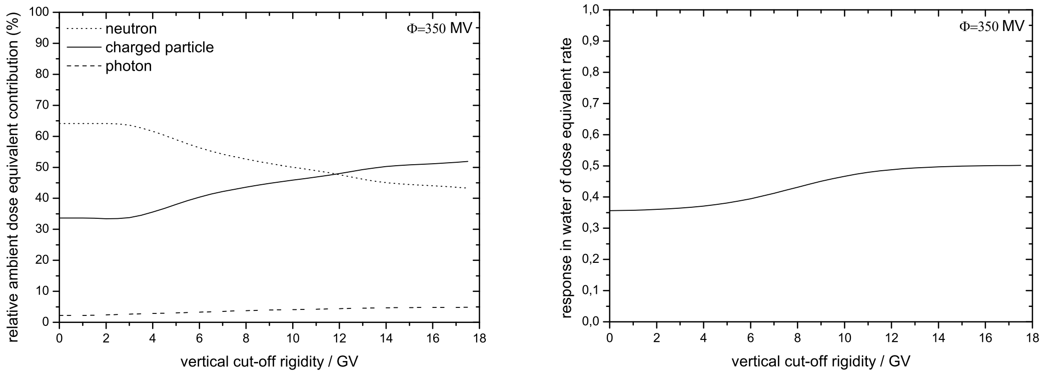

Fig. 4. Plot on the left side: Relative composition of the radiation field components which contribute to the ambient dose equivalent rate at FL350 near solar minimum conditions ($\Phi = 350$ MV), as calculated with EXPACS (Sato, 2006, 2008). The solid, dotted and dashed lines show the contributions of neutrons, charged particles and photons, respectively. The plot on the right hand shows the instrument response calculated by the reciprocal of the calibration function of Eq. (2) (solid line).

Since EXPACS calculates the dose rate in tissue equivalent material we need to determine $\dot{D}_{\mathrm{water}}$ as described above. Figure 4 (right plot) shows the ratio of $\dot{D}_{\mathrm{water}}$ and $\dot{H}^*(10)$ derived from the fitted field function N_{fit} (see Eq. 2):

$$\frac{\dot{D}_{\mathrm{water}}}{\dot{H}^*(10)_{\mathrm{FD}}} = \frac{F_{\mathrm{Si-water}}}{N_{\mathrm{fit}}(R_{\mathrm{c}})}\,. \quad (5)$$

Note, $\frac{1}{N_{\mathrm{fit}}(R_{\mathrm{c}})}$ has to be multiplied by $F_{\mathrm{Si-water}}$ in order to take into account the different stopping power in water compared to silicon. Substituting $N_{\mathrm{fit}}(R_{\mathrm{c}})$ by the quantities defined in Eq. (4) one obtaines

$$\frac{\dot{D}_{\mathrm{water}}}{\dot{H}^*(10)_{\mathrm{FD}}} = \frac{1}{C_{\mathrm{field}}(R_{\mathrm{c}})} \quad (6)$$

The latter quantity as a function of the vertical cut-off rigidity R_{c} is displayed in Fig. 4 right. By comparing the shape of the charged particle contribution to the total dose rate in Fig. 4 left from EXPACS with $\frac{1}{C_{\mathrm{field}}(R_{\mathrm{c}})}$ we find a close similarity. Thus we conclude that (1) DOSTEL is mainly sensitive to charged particles and that (2) the calibration function corrects for this deficiency. Figure 5 displays a comparison from the same ratios as in Fig. 4 for solar minimum condition (heliocentric potential $\Phi = 283$ MV) and maximum conditions ($\Phi = 1125$ MV) (Usoskin, 2011). The comparison shows that the neutron and the charged particle component of the dose equivalent rate will be changed during the solar cycle. This effect is very small in the equator region ($R_{\mathrm{c}} > 10$ GV) and, therefore, can be neglected in this region. In the polar region ($R_{\mathrm{c}} < 3$ GV) and in the intermediate region the solar cycle must be considered for a precise determination of the dose equivalent rate and the calibration function has to be reviewed for other solar conditions. But for an estimation of the dose equivalent rate the calibration function can extrapolated for the whole solar cycle.

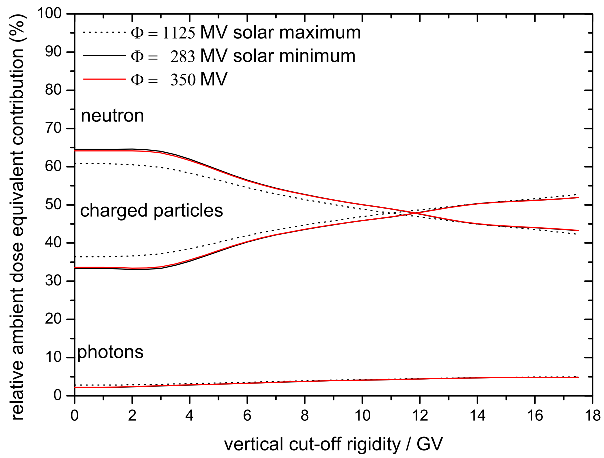

Fig. 5. The relative composition of the ambient dose equivalent rate on FL350 for solar minimum and maximum conditiond as calculated with EXPACS. The solid line displays the dose rate composition for the solar minimum ($\Phi = 283$ MV) and the dotted line for solar maximum conditions ($\Phi = 1125$ MV). The red curves correspond to the solar activity during the measurements (Φ=350 MV).

5 Conclusions

Here we showed that DOSTEL can be used as dosemeter on board an aircraft. Therefore we calibrated it in terms of ambient dose equivalent. This calibration resulted from intercomparison flights. Furthermore these flights proved that FDOScalc is usable for in-flight calibration because the comparison with the πDOS showed a good agreement. The calibration shows a strong dependence on the vertical cut-off rigidity due to the changes in the composition of the radiation field. The comparison with the PARMA code using EXPACS demonstrates that NAVIDOS is measuring mainly charged particles and that the calibration function corrects the part of the neutron dose. The calibration function has to be reviewed over the solar cycle because the field conditions will change. But for an estimation of the ambient dose equivalent rate the calibration function is usable.

Acknowledgements. For their support to organize the flights to Cape Town (with DLH) and to Bangkok (with LTU) we thank J. Briese (DLH), M. Nezel and F. Luchtenberg (both LTU).

We would like to express our gratitude to K. Herbst (CAU) for the calculation of the 5° × 5° grid of vertical cut-off rigidities.

For doing excellent measurements during the additional flights we appreciate the intense work of Th. Klages and F. Langner (all PTB).

A part of the work done by PTB was supported by the Federal Ministry for Transport, Building and Urban Affairs (project FV 50.0320/2006).

Edited by: H. Fichtner
Reviewed by: four anonymous referees

References

Bartlett, D. T.: Radiation Protection Aspects of Cosmic Radiation Exposure of Aircraft Crew, Radiat. Prot. Dosimetry, 109, 349–355, 2004.

Beaujean, R., Kopp, J., and Reitz, G.: Radiation exposure in Civil Aircraft, Radiat. Prot. Dosimetry, 85, 287–290, 1999a.

Beaujean, R., Kopp, J., and Reitz, G.: Active Dosimetry on Recent Space Flight, Radiat. Prot. Dosimetry, 85, 223–226, 1999b.

Beaujean, R., Burmeister, S., Petersen, F., and Reitz, G.: Radiation Exposure Onboard Civil Aircraft, Radiat. Prot. Dosimetry, 116, 312–315, 2005.

Benton, E. R., Benton, E. V., and Frank, A. L.: Conversion between different forms of LET, Radiation Measurements, 45, 957–959, 2010.

Büermann, L., Guldbakke, S., and Kramer, H.-M.: Calibration of personal and area dosimeters in high-energy photon fields, PTB-Bericht PTB-Dos-32, Braunschweig, ISBN 3-897001-285-5, 1999.

International Commission on Radiation Units and Measurement, Stopping Powers for Electrons and Protons, Report 37 (Bethesda, MD:ICRU), 1984.

Lewis, B. J., Bennett, L. G. I.,Green, A. R., McCall, M. J.,Ellaschuk, B., Butler, A., and Pierre, M.: Galactic and Solar Radiation Exposure to Aircrew During a Solar Cycle, Radiat. Prot. Dosimetry, 102, 207–227, 2002.

Möller, T.: Charakterisierung eines Dosimeters zur Messung der Ortsdosisleistung in Flughöhen, Diploma Thesis, University of Kiel, 2008.

Nolte, R., Allie, M. S., Böttger, R. , Brooks, F. D., Buffler, A. , Dangendorf, V. , Friedrich, H. , Guldbakke, S., Klein, H. , Meulders, J. P. , Schlegel, D., Schuhmacher, H., and Smit F. D.: Quasi-monoenergetic Neutron Reference Fields in the Energy Range from Thermal to 200 MeV, Radiat. Prot. Dosimetry, 110, 97–102, 2004.

The Oulu (Finland) neutron monitor data can be accessed via http://cosmicrays.oulu.fi, 2008.

Roos, F.: Messung der Strahlenexposition in Verkehrsflugzeugen mit einem Halbleiterdetector, Diploma Thesis, 1997.

Radio Technical Commission for Aeronautics, Document DO-160D Environmental conditions and test procedures for airborne equipment, Washington, 1997.

Sato, T. and Niita, K.: Analytical Functions to Predict Cosmic-Ray Neutron Spectra in the Atmosphere, Radiat. Res., 166, 544–555, 2006.

Sato, T., Endo, A., and Nita, K.: Development of PARMA: PHITS-based Analytical Radiation Model in the Atmosphere, Radiat. Res., 170, 244–259, 2008.

Schrewe, U. J.: Global Measurements of the Radiation Exposure of Civil Air Crew from 1997 to 1999, Radiat. Prot. Dosimetry, 91, 347–364, 2000.

Usoskin, I. G., Bazilevskaya, G. A., and Kovaltsov, G. A.: Solar Modulations Parameter for Cosmic Rays Since 1936 Reconstructed From Ground-based Neutron Monitors and Ionization Chambers, J. Geophys. Res., 116, A02104, doi:10.1029/2010JAO16105, 2011.

Wissmann, F., Langner, F., Roth, J., and Schrewe, U.: A Mobile TEPC-Based System to Measure the Contributions to $H^*(10)$ at Flight Altitudes, Radiat. Prot. Dosimetry, 110, 347–349, 2004.

Wissmann, F.: Long-term Measurements of $\dot{H}^*(10)$ at Aviation Altitudes in the Northern Hemisphere, Radiat. Prot. Dosimetry, 121, 347, 2006.

Wissmann, F., Reginatto, M., and Möller, T.: Ambient Dose Equivalent at Flight Altitudes: A Fit to a Large Set of Data using a Bayesian Approach, J. Radiol. Prot., 30, 513, 2010a.

Wissmann, F., Burmeister, S., Hubiak, M., Heber, B., Klages, T., Langner, F., Möller,T., and Meier, M.: Field calibration of dosemeters used for routine measurements at flight altitudes, Radiat. Prot. Dosimetry, 140, 319–325, 2010b.